Title

Engagement of Foxh1 in chromatin regulation revealed by protein interactome analyses

Journal

Development Growth & Differentiation, 64(6)

ISSN

0012-1592

Authors

Zhou, Jeff Jiajing

Pham, Paula Duyen

Han, Han

et al.

Publication Date

2022-08-01

DOI

10.1111/dgd.12799

Peer reviewed

Published in final edited form as:

Dev Growth Differ. 2022 August ; 64(6): 297–305. doi:10.1111/dgd.12799.

Foxh1 engages in chromatin regulation revealed by protein interactome analyses

Jeff Jiajing Zhou[1], **Paula Duyen Pham**[1], **Han Han**[1], **Wenqi Wang**[1], **Ken W.Y. Cho**[1,2,3,*]

[1]Department of Developmental and Cell Biology, University of California, Irvine, Irvine, CA, 92697, USA

[2]Center for Complex Biological Systems, University of California, Irvine, CA, USA

[3]Lead Contact

Abstract

Early embryonic cell fates are specified through coordinated integration of transcription factor activities and epigenetic states of the genome. Foxh1 is a key maternal transcription factor controlling the mesendodermal gene regulatory program. Proteomic interactome analyses using FOXH1 as a bait in mouse embryonic stem cells revealed that FOXH1 interacts with PRC2 subunits and HDAC1. Foxh1 physically interacts with Hdac1, and confers transcriptional repression of mesendodermal genes in *Xenopus* ectoderm. Our findings reveal a central role of Foxh1 in coordinating the chromatin states of the *Xenopus* embryonic genome.

Keywords

Xenopus; pioneer transcription factors; HDAC; PRC2; epigenetics; proteomics

Introduction

Early embryos undergo drastic genetic reprogramming accompanied by epigenetic remodeling to robustly establish various embryonic cell fates. Extensive studies have identified many essential genes that confer either positive or negative regulation on developmental programs (ENCODE Project Consortium 2012& 2020). In *Xenopus*, Foxh1, a maternal forkhead-box transcription factor (TF), is a critical cofactor in forming a nodal-induced Smad-Foxh1 complex that directs mesodermal and endodermal cell lineages (Zhou et al., 1998; Hill, 2001; Whitman, 2001; Howell et al., 2002; Kofron et al., 2004; Chiu et al., 2014). Foxh1 binds to embryonic genome as early as the 32~64 cell stage, which is significantly earlier than the first major wave of zygotic genome activation (ZGA) (Charney et al., 2017). Time-course ChIP-seq analyses revealed that Foxh1 persistently binds to many putative mesendodermal *cis*-regulatory modules, which subsequently gain well-characterized active histone modifications such as H3K4me1 and H3K27ac during ZGA and onward. These observations raise the question of whether Foxh1 directly recruits epigenetic modifiers like histone-modifying enzymes during ZGA.

*Correspondence: kwcho@uci.edu (K.W.Y.C.).

In this study, we characterize FOXH1-associated protein complexes in mouse embryonic stem cells (mESCs) through a proteomic approach. Our data suggest that Foxh1-interacting proteins can regulate gene expression by altering chromatin architectures. Among them, the protein-protein interactions between Foxh1-PRC2 core subunits and Foxh1-Hdac1 appear to be notable. We highlight that Foxh1 and Hdac1 co-repress a small subset of mesendodermal genes in the ectoderm during *Xenopus* germ layer specification, suggesting the role of Foxh1 in safeguarding misactivation of mesendodermal genes in the ectoderm.

Materials and Methods

DNA plasmid constructs

Mouse FOXH1 cDNA (F: ATGGCCTCGGGCTGGGACCT, R: TTACATGCTGTACCAGGAAAGGAGCCAGCCT) was cloned into the destination vector containing *C*-terminal triple (S tag-Flag tag-SBP tag, or SFB) tags (Wang et al., 2014). The resulting mFOXH1-SFB is cloned into pLV-EF1a-IRES-Puro (Addgene, 85132) for lentivirus production. Ezh2 (F: ATGGGCCAGACGGGCAAGAA, R: TCAGGGGATTTCCATTTCTCTCTCAATACC), Eed (F: ATGTCCGAAGCTTCCGGTC, R: TCACCGCAGTCTGTCCCAG), Suz12 (F: ATGGCCCCTCAGAAGCACG, R: TCAGGGCTTCTGCTTTTTGCTGT), Hdac1 (F: ATGGCGCTGAGTCAAGGA, R: TCAGGCAGATTTGGTCTCT) cDNAs were cloned into pCS2+ (modified from Addgene 102860) to generate HA tagged fusion proteins. Foxh1 cDNA (F: ATGAGAGACCCCTCCAGTCTG, R: CTACATTAGACCTTGCCTGCTTGG) was cloned in pCS2+ to generate 3X FLAG tagged fusion protein.

Cell culture and Lentiviral transduction

E14 mESC cells were cultivated in KnockOut D-MEM with FBS, GlutaMAX (Thermo Fisher), MEM non-essential amino acids, penicillin-streptomycin, b-mercaptoethanol, and murine LIF (Millipore Sigma). Lentivirus containing pLV-EF1a-mFOXH1-SFB-IRES-Puro was packaged by psPAX2 (Addgene) and pMD2.G (Addgene), and transduced on mESCs. Puromycin (5ug/ml) was applied consecutively to select target clones. After 14 days, single clones were expanded. HEK293T cells were cultured in DMEM with FBS and penicillin-streptomycin. HEK293T cells were transfected with polyethylenimine (Longo et al., 2013).

Animal Model and Morpholinos

Xenopus tropicalis embryos were fertilized and cultured in 1/9X Marc's modified Ringers. Embryos were dissected at the late blastula stage (6 hpf) and cultured to the early gastrula (7 hpf) for harvest. Foxh1 morpholino injections were performed at the 1-cell stage. 22.5 ng of *foxh1* (*foxh1* MO: 5′-TCATCCTGAGGCTCCGCCCTCTCTA-3′; Chiu et al., 2014) or standard control (Genetools) was used. For a rescue experiment, *foxh1* MO and *in vitro* transcribed *foxh1* mRNA (30 pg) from pCS2-3X FLAG-foxh1 were co-injected into an embryo.

Immunoprecipitation and co-Immunoprecipitation

For mFOXH1 mass spectrometry, 3×10^7 mFOXH1 mESCs were harvested and followed as described (Wang et al., 2014). The purification eluate was analyzed by Harvard Taplin MS

facility for LC-MS. For co-immunoprecipitation, transfected cells were lysed in cell lysis buffer and subjected to IP using anti-FLAG (Millipore-Sigma) or anti-HA (Millipore-Sigma) with Pierce protein A/G magnetic beads (Thermo Scientific). Beads were washed with lysis buffer, followed by the elution using 2X SDS loading buffer. The protein eluate was analyzed using western blotting. For benzonase treatment, 100 units of benzonase (Sigma-Aldrich) were added to each IP sample. The final concentrations of ethidium bromide used are 50, 100 and 400ng/ul for each IP sample.

Western Blotting

Cells were directly harvested in 1X SDS loading buffer, boiled at 95°C, and subjected to western blotting using anti-FLAG, anti-Tubulin (Sigma, T5168), and anti-HA.

Immunofluorescence

Cells were fixed in 4% paraformaldehyde for 10 min at room temperature (RT), permeabilized with 0.5% Triton X-100 in PBS for 5 min, and then blocked with 0.1% Tween-20 (in TBST) and 2% Goat Serum (Vector Laboratories, NC9270494) for 1h at RT. A dilution of 1:200 anti-FLAG (Millipore-Sigma) antibody was incubated with cells for 1h at RT, and washed three times with TBST. Cells were incubated with AlexaFluor488 (Thermo Fisher) for 1h, washed three times in TBST, and stained with Hoechst (Sigma). Confocal images were acquired using the Nikon A1R point scanning confocal microscope.

Gene Expression Analysis and RNA-seq

For RT-qPCR, reverse-transcription assays were performed using Maxima reverse transcriptase (Thermo Fisher). RT-qPCR was performed using LightCycler 480 SYBR Green I master mix (Roche). RT-qPCR primer sequences are as follow. *Eomes* F: ACCGGCACCAAACTGAGA, R: AAGCTCAAGAAAGGAAACATGC; *Foxa2* F: CCATCAGCCCCACAAAATG, R: CCAAGCTGCCTGGCATG; *Foxh1* F: ATTATCCGTCAGGTCCAGGC, R: TAGAGGAAAGGTTGTGGCGG; *Nanog* F: CCAACCCAACTTGGAACAAC, R: TATGGAGCGGAGCAGCAT; *Oct4* F: TTGCAGCTCAGCCTTAAGAAC, R: TCATTGTTGTCGGCTTCCCT; *Pax6* F: CACCAGACTCACCTGACACC, R: ACCGCCCTTGGTTAAAGTC; *Tbxt* F: CAGCCCACCTACTGGCTCTA, R: GAGCCTGGGGTGATGGTA. For quantification of gene expression, the 2^ −ΔΔCt method was used. *gapdh* was used as a control gene for normalization. For RNA-seq, total RNA from dissected animal cap explants was extracted using Trizol (Amin et al., 2014). mRNA was isolated using NEBNext PolyA mRNA Magnetic Isolation Module. Sequencing libraries were prepared using NEBNext Ultra II RNA library prep kit and sequenced by the Illumina NovaSeq 6000. All experiments were done in 2 biological replicates. Sequencing samples were aligned using STAR v2.7.3a (Dobin et al., 2013) to *Xenopus tropicalis* genome v10.0 (http://www.xenbase.org/, RRID:SCR_003280). Differentially expressed genes were identified using edgeR v3.36.0 (Robinson et al., 2010) with parameters fold change >2 and false discovery rate (FDR) < 0.05 in R v4.1.2 (R Core Team, 2022). Gene ontology analysis was performed using Metascape (Zhou et al., 2019) with default parameters (min overlap= 3, p-value cutoff= 0.01, and min enrichment= 1.5) and visualized by Cytoscape (Shannon et al., 2003).

Additional Analysis

Mass spectrometry: List of proteins detected in three independent spectrometry experiments (using heterogeneous pooled, monoclonal 1, and monoclonal 2 cells) were compared, and overlapping proteins were identified after removing identified proteins from the negative control (wildtype E14 mESCs). Spatial expression analysis: Sequencing data from dissected *Xenopus* gastrula embryonic tissues (Blitz et al., 2017) were aligned using STAR v2.7.3a (Dobin et al., 2013) and quantified by RSEM v1.3.3 (Li and Dewey, 2011) to obtain TPM values. TPMs for marginal zones were calculated as the mean TPMs of dorsal, lateral and ventral marginal zones. ChIP-seq: Sequencing data were aligned to *Xenopus* tropicalis v10.0 genome (http://www.xenbase.org/, RRID:SCR_003280) using Bowtie2 v2.4.4 (Langmead and Salzberg, 2012). PCR duplicates were removed using Samtools v1.10 (Li et al., 2009). Irreproducibility discovery rate (IDR) analysis (Li et al., 2011) was used to identify high-confidence peaks called by Macs2 v2.7.1 (Zhang et al., 2008) between two biological replicates following ENCODE3 ChIP-seq pipelines (IDR threshold of 0.05). Clusters are made by Bedtools v2.29.2 (Quinlan and Hall, 2010). Clustered heatmaps were generated using DeepTools v3.5.0 (Ramírez et al., 2014). Genes suppressed by Hdac1: The gene list is obtained by overlapping an up-regulated gene list (855 genes) after HDAC inhibition in the ectoderm and a gene list (10,683 genes) bound by Hdac1 at early gastrula stage (Zhou et al., BioRxiv 2022).

Data Accessibility

RNA-seq datasets generated from this study are available at NCBI Gene Expression Omnibus using GSE204990. Publicly available datasets used are available at NCBI GEO: GSE53654 (Foxh1 ChIP-seq), GSE85273 (Foxh1 ChIP-seq), GSE81458 (RNA-seq of regionally isolated gastrula tissues), GSE198378 (Hdac1 ChIP-seq, HDAC inhibition RNA-seq).

Results and Discussion

Generation of E14 cells stably expressing protein mFOXH1-SFB

To minimize interference from large amounts of yolk granules present in *Xenopus* embryos, we generated E14 mESC lines stably expressing mFOXH1 with epitope tags encoding S-protein peptide, two FLAG peptides, and a streptavidin-binding peptide (SBP) (Wang et al., 2014) (Figure 1A). The S-protein peptide and SBP tags enable a sequential pulldown, while the FLAG tag allows for the detection of bait protein. A population of E14 cells transduced with lentivirus harboring mFOXH1-SFB were expanded, and shown to express mFOXH1-SFB (Figure 1B, 1C). This population of mFOXH1-SFB E14 mESCs consists of a heterogeneous pool of cells with different integration sites and copies of mFOXH1-SFB. Immunofluorescence staining of mFOXH1-SFB showed localized expression in the nucleus (Figure 1D). Clonally expanded mFOXH1-SFB E14 mESCs (monoclonal 1 and 2) exhibited more uniform expression of mFOXH1-SFB protein. Variable protein levels of mFOXH1-SFB were expressed in different clones of mFOXH1-SFB E14 mESCs (Figure 1E). Gene expression analyses showed high levels of mFoxh1 and pluripotency gene transcripts (e.g., *Nanog*), but not early germ layer marker gene transcripts (e.g., *Tbxt*, *Eomes* and *Foxa2*),

suggesting that mFoxh1 overexpression does not affect the cellular pluripotency of mESCs (Figure 1F).

FOXH1 participates in diverse chromatin regulation

Liquid chromatography-mass spectrometry (LC-MS) was performed on mFOXH1-SFB purification eluate. A total of 342 proteins consistently recovered from three independent samples (heterogeneous pool, monoclonal 1, and monoclonal 2 cells) are considered as putative mFOXH1 interactants (Table 1). Gene ontology enrichment analysis showed that mFOXH1 participates in diverse cellular processes (Figure 2A). We highlight that mFOXH1 interacts with proteins functioning in various aspects of chromatin regulation (Figure 2B), consistent with the notion that some critical TFs often recruit coregulators to influence the local chromatin states (Spitz and Furlong, 2012; Chen and Dent, 2013; Zaret, 2020). SMAD2 and SMAD3, known FOXH1 interactants through Activin/Nodal signaling (Massagué, 2012), are captured. Proteins positively or negatively regulating chromatin are identified as potential mFOXH1 interacting proteins (Figure 2C). For example, SMARCA5 and HELLS are known regulators related to SWI-SNF chromatin remodeling complexes (Oppikofer et al., 2017; Dennis et al., 2001). NSD1 is a histone methyltransferase depositing H3K36 methylation during transcription elongation (Lucio-Eterovic et al., 2010). TET1 and OGT are assembled into DNA methyltransferase complexes (Hrit et al., 2018). SUZ12, JARID2, and EZH2 are subunits of Polycomb repressive complex 2 (PRC2) that deposits H3K27me3 modification on inactive genes (Chammas et al., 2019). HDAC1 is a histone deacetylase removing active histone acetylation modifications (Seto and Yoshida, 2014). These results suggest that mFOXH1 participates in diverse epigenetic processes which can either positively or negatively regulate transcription.

To confirm that similar interactions identified in mESCs can also occur among *Xenopus* counterparts, we performed co-immunoprecipitation (co-IP) experiments using respective *Xenopus* protein counterparts. To distinguish DNA/RNA-dependent and -independent association of these proteins, protein lysates were treated with either ethidium bromide to disrupt the structure of nucleic acids or Benzonase endonuclease to degrade nucleic acids. We showed that Foxh1 physically interacts with three core subunits (Ezh2, Eed, and Suz12) of PRC2 (Figure 2D). The interaction between Foxh1 and Hdac1 was also confirmed (Figure 2E). These validation studies suggest that *Xenopus* Foxh1 functions as a transcriptional repressor via the recruitment of PRC2 and Hdac1-containing complexes.

The role of Foxh1 in developing embryonic ectoderm

Nodal signaling is only active vegetally, whereas Foxh1 is expressed uniformly in early embryos. We speculate that Foxh1 bears a repressive function in the absence of Nodal signaling within the ectoderm. We tested the model whereby Foxh1 recruits a repressive epigenetic modifier Hdac1 to repress mesendodermal genes in the developing ectoderm.

First, we identified genes regulated by Foxh1 in the ectoderm. *Xenopus* embryos were injected with control or Foxh1 morpholino (MO) animally, and developed until the late blastula stage. Animal cap (prospective ectoderm) tissues were dissected and incubated to the early gastrula equivalent stage for RNA-seq (Figure 3A). Foxh1 morphants

exhibited incomplete blastopore closure and impaired AP axis (80%, n=10 embryos). These abnormalities are partially rescued (70%, n=10) by ectopic expression of MO-resistant *foxh1* mRNA in Foxh1 morphants (Figure 3B). Differential gene expression analysis of ectodermal tissues isolated from Foxh1 morphant and control embryos revealed 192 upregulated and 384 downregulated genes (Figure 3C). Spatial gene expression analyses (Blitz et al., 2017) comparing animal (ectoderm), marginal (mesoderm) and vegetal (endoderm) tissue fragments showed that differentially regulated genes by Foxh1 in ectoderm do not exhibit any germ layer enrichment (Figure 3D). Next, we examined the biological function of Foxh1-Hdac1 interaction. Foxh1and Hdac1 share similar binding profiles (Figure 3E), suggesting that Foxh1 and Hdac1 occupy similar genomic regions. A list of 513 Hdac1 suppressed genes were identified through combined analyses on genes induced after HDAC inhibitor (Trichostatin A, TSA) and Hdac1 bound genes (Zhou et al., BioRxiv 2022). Of 192 Foxh1 repressed genes, 12 genes were suppressed by Hdac1 (Figure 3F). Notably, 11 of the 12 Foxh1-Hdac1 co-repressed genes showed enriched expression in either mesoderm or endoderm, suggesting that Foxh1 and Hdac1 co-repress mesendodermal genes in the ectoderm. That a small percentage (6.3%) of genes are suppressed by Foxh1-Hdac1 indicates additional mechanisms (i.e., the involvement of other TFs for Hdac1 recruitment in the absence of Foxh1) playing a role in inhibiting the expression of other mesendodermal genes in the developing ectoderm (Figure 3G).

In sum, our FOXH1 proteomic study identified epigenetic modifiers involved in different aspects of chromatin regulations (Figure 2B, 2C). The capture of SMARCA5 and HELLS, regulators related to SWI/SNF complex, provides a mechanism where Foxh1 may exploit the activity of SWI/SNF complex to alter nucleosome positions along the early embryonic genome. Foxh1 physically interacts with both PRC2 (Figure 2D) and Hdac1 (Figure 2E), presumably conferring repressive chromatin states through H3K27me3 deposition and histone hypoacetylation. We propose that the interaction between Foxh1 and Hdac1 occurs in the physiological context, causing transcriptional repression in the ectoderm of developing embryos (Figure 3G) based on the following evidence. Nodal signaling is absent in the ectoderm (Hill et al., 2001) while Foxh1 is ubiquitously expressed (Chiu et al., 2014; Charney et al., 2017) in early *Xenopus* embryos. Foxh1 physically interacts with PRC2 subunits and Hdac1 (Figure 2D, 2E). The genomic binding profile of Hdac1 highly overlaps with that of Foxh1 (Figure 3E). Importantly, 11 out of 12 Foxh1-Hdac1 co-repressed genes in the ectoderm (Figure 3F) are expressed in the mesoderm and endoderm. This supports the model that Foxh1 functions as a transcriptional repressor for mesendodermal genes in the ectoderm via the histone deacetylase activity of Hdac1. Since only a subset of Foxh1 target genes are affected by HDAC inhibition, it is tempting to speculate that other TFs function in a combinatory fashion (Ravasi et al., 2010). In light of the model, our previous studies in *Xenopus* showed that Foxh1 binds to genomic regions overlapped with multiple TFs such as Otx1, Vegt, Sox3, and Sox7 (Paraiso et al., 2019; Jansen et al., 2022; Zhou et al., BioRxiv 2022). Hence, a loss or reduction of Foxh1 alone may be insufficient to fully relieve this suppression. It will be useful to determine whether these maternal TFs function cooperatively with Foxh1 to suppress mesendodermal genes in the ectoderm.

Acknowledgments

We thank current Cho lab members for critical comments, the Genomic High Throughput Facility at University of California, Irvine for sequencing services, Xenbase (RRID:SCR_003280) for genomic and community resources, the National Xenopus Resource (RRID:SCR_013713) for *Xenopus tropicalis*, and Taplin Mass Spectrometry Facility at Harvard Medical School for LC-MS services. This work is supported by NIH R01GM126395, R35GM139617 and NSF 1755214 to K.W.Y.C., and NIH R01GM126048 and ACS RSG-18-009-01-CCG to W.W..

Reference

Amin NM, Tandon P, Osborne Nishimura E, Conlon FL. RNA-seq in the tetraploid *Xenopus laevis* enables genome-wide insight in a classic developmental biology model organism. Methods. 2014 Apr 1;66(3):398–409. [PubMed: 23792920]

Blitz IL, Paraiso KD, Patrushev I, Chiu WTY, Cho KWY, Gilchrist MJ. A catalog of *Xenopus* tropicalis transcription factors and their regional expression in the early gastrula stage embryo. Dev Biol. 2017 Jun 15;426(2):409–417. [PubMed: 27475627]

Chammas P, Mocavini I & Di Croce L Engaging chromatin: PRC2 structure meets function. Br J Cancer 122, 315–328 (2020). [PubMed: 31708574]

Charney RM, Forouzmand E, Cho JS, Cheung J, Paraiso KD, Yasuoka Y, Takahashi S, Taira M, Blitz IL, Xie X, Cho KW. Foxh1 Occupies *cis*-Regulatory Modules Prior to Dynamic Transcription Factor Interactions Controlling the Mesendoderm Gene Program. Dev Cell. 2017 Mar 27;40(6):595–607.e4. [PubMed: 28325473]

Chen T, Dent SY. Chromatin modifiers and remodellers: regulators of cellular differentiation. Nat Rev Genet. 2014 Feb;15(2):93–106. [PubMed: 24366184]

Chiu WT, Charney Le R, Blitz IL, Fish MB, Li Y, Biesinger J, Xie X, Cho KW. Genome-wide view of TGFβ/Foxh1 regulation of the early mesendoderm program. Development. 2014 Dec;141(23):4537–47. [PubMed: 25359723]

Dennis K, Fan T, Geiman T, Yan Q, Muegge K. Lsh, a member of the SNF2 family, is required for genome-wide methylation. Genes Dev. 2001 Nov 15;15(22):2940–4. [PubMed: 11711429]

Dobin A, Davis CA, Schlesinger F, Drenkow J, Zaleski C, Jha S, Batut P, Chaisson M, Gingeras TR. STAR: ultrafast universal RNA-seq aligner. Bioinformatics. 2013 Jan 1;29(1):15–21. [PubMed: 23104886]

ENCODE Project Consortium, Moore JE, Purcaro MJ, Pratt HE, Epstein CB, Shoresh N, Adrian J, Kawli T, Davis CA, et al. Expanded encyclopaedias of DNA elements in the human and mouse genomes. Nature. 2020 Jul;583(7818):699–710. [PubMed: 32728249]

ENCODE Project Consortium. An integrated encyclopedia of DNA elements in the human genome. Nature. 2012 Sep 6;489(7414):57–74. [PubMed: 22955616]

Fortriede JD, Pells TJ, Chu S, Chaturvedi P, Wang D, Fisher ME, James-Zorn C, Wang Y, Nenni MJ, Burns KA, et al. Xenbase: deep integration of GEO & SRA RNA-seq and ChIP-seq data in a model organism database. Nucleic Acids Res. 2020 Jan 8;48(D1):D776–D782. [PubMed: 31733057]

Hill CS. TGF-beta signalling pathways in early *Xenopus* development. Curr Opin Genet Dev. 2001 Oct;11(5):533–40. [PubMed: 11532395]

Howell M, Inman GJ, Hill CS. A novel *Xenopus* Smad-interacting forkhead transcription factor (XFast-3) cooperates with XFast-1 in regulating gastrulation movements. Development. 2002 Jun;129(12):2823–34. [PubMed: 12050132]

Hrit J, Goodrich L, Li C, Wang BA, Nie J, Cui X, Martin EA, Simental E, Fernandez J, Liu MY, Nery JR, Castanon R, Kohli RM, Tretyakova N, He C, Ecker JR, Goll M, Panning B. OGT binds a conserved C-terminal domain of TET1 to regulate TET1 activity and function in development. Elife. 2018 Oct 16;7:e34870. [PubMed: 30325306]

Jansen C, Paraiso KD, Zhou JJ, Blitz IL, Fish MB, Charney RM, Cho JS, Yasuoka Y, Sudou N, Bright AR, Wlizla M, Veenstra GJC, Taira M, Zorn AM, Mortazavi A, Cho KWY. Uncovering the mesendoderm gene regulatory network through multi-omic data integration. Cell Rep. 2022 Feb 15;38(7):110364. [PubMed: 35172134]

Kofron M, Puck H, Standley H, Wylie C, Old R, Whitman M, Heasman J. New roles for FoxH1 in patterning the early embryo. Development. 2004 Oct; 131(20):5065–78. [PubMed: 15459100]

Langmead B, Salzberg SL. Fast gapped-read alignment with Bowtie 2. Nat Methods. 2012 Mar 4;9(4):357–9. [PubMed: 22388286]

Li B, Dewey CN. RSEM: accurate transcript quantification from RNA-Seq data with or without a reference genome. BMC Bioinformatics. 2011 Aug 4;12:323. [PubMed: 21816040]

Li H, Handsaker B, Wysoker A, Fennell T, Ruan J, Homer N, Marth G, Abecasis G, Durbin R; 1000 Genome Project Data Processing Subgroup. The Sequence Alignment/Map format and SAMtools. Bioinformatics. 2009 Aug 15;25(16):2078–9. [PubMed: 19505943]

Li Q, Brown JB, Huang H, and Bickel PJ (2011). Measuring reproducibility of high- throughput experiments. Ann. Appl. Stat 5, 1752–1779.

Longo PA, Kavran JM, Kim MS, Leahy DJ. Transient mammalian cell transfection with polyethylenimine (PEI). Methods Enzymol. 2013;529:227–40. [PubMed: 24011049]

Lucio-Eterovic AK, Singh MM, Gardner JE, Veerappan CS, Rice JC, Carpenter PB. Role for the nuclear receptor-binding SET domain protein 1 (NSD1) methyltransferase in coordinating lysine 36 methylation at histone 3 with RNA polymerase II function. Proc Natl Acad Sci U S A. 2010 Sep 28;107(39):16952–7. [PubMed: 20837538]

Massagué J. TGFβ signalling in context. Nat Rev Mol Cell Biol 13, 616–630 (2012). [PubMed: 22992590]

Oppikofer M, Bai T, Gan Y, Haley B, Liu P, Sandoval W, Ciferri C, Cochran AG. Expansion of the ISWI chromatin remodeler family with new active complexes. EMBO Rep. 2017 Oct;18(10):1697–1706. [PubMed: 28801535]

Paraiso KD, Blitz IL, Coley M, Cheung J, Sudou N, Taira M, Cho KWY. Endodermal Maternal Transcription Factors Establish Super-Enhancers during Zygotic Genome Activation. Cell Rep. 2019 Jun 4;27(10):2962–2977.e5. [PubMed: 31167141]

Quinlan AR, Hall IM. BEDTools: a flexible suite of utilities for comparing genomic features. Bioinformatics. 2010 Mar 15;26(6):841–2. [PubMed: 20110278]

R Core Team (2022). R: A language and environment for statistical computing. R Foundation for Statistical Computing, Vienna, Austria. URL https://www.R-project.org

Ramírez F, Dündar F, Diehl S, Grüning BA, Manke T. deepTools: a flexible platform for exploring deep-sequencing data. Nucleic Acids Res. 2014 Jul;42(Web Server issue):W187–91. [PubMed: 24799436]

Ravasi T, Suzuki H, Cannistraci CV, Katayama S, Bajic VB, Tan K, Akalin A, Schmeier S, Kanamori-Katayama M, Bertin N, et al. An atlas of combinatorial transcriptional regulation in mouse and man. Cell. 2010 Mar 5;140(5):744–52. [PubMed: 20211142]

Robinson MD, McCarthy DJ, Smyth GK. edgeR: a Bioconductor package for differential expression analysis of digital gene expression data. Bioinformatics. 2010 Jan 1;26(1):139–40. [PubMed: 19910308]

Seto E, Yoshida M. Erasers of histone acetylation: the histone deacetylase enzymes. Cold Spring Harb Perspect Biol. 2014 Apr 1;6(4):a018713. [PubMed: 24691964]

Shannon P, Markiel A, Ozier O, Baliga NS, Wang JT, Ramage D, Amin N, Schwikowski B, Ideker T. Cytoscape: a software environment for integrated models of biomolecular interaction networks. Genome Res. 2003 Nov;13(11):2498–504. [PubMed: 14597658]

Spitz F, Furlong EE. Transcription factors: from enhancer binding to developmental control. Nat Rev Genet. 2012 Sep;13(9):613–26. [PubMed: 22868264]

Wang W, Li X, Huang J, Feng L, Dolinta KG, Chen J. Defining the protein-protein interaction network of the human hippo pathway. Mol Cell Proteomics. 2014 Jan;13(1):119–31. [PubMed: 24126142]

Whitman M. Nodal signaling in early vertebrate embryos: themes and variations. Dev Cell. 2001 Nov;1(5):605–17. [PubMed: 11709181]

Zaret KS. Pioneer Transcription Factors Initiating Gene Network Changes. Annu Rev Genet. 2020 Nov 23;54:367–385. [PubMed: 32886547]

Zhang Y, Liu T, Meyer CA, Eeckhoute J, Johnson DS, Bernstein BE, Nusbaum C, Myers RM, Brown M, Li W, Liu XS. Model-based analysis of ChIP-Seq (MACS). Genome Biol. 2008;9(9):R137. [PubMed: 18798982]

Zhou JJ, Cho JS, Han H, Blitz IL, Wang W, Cho KWY. Histone deacetylase 1 maintains lineage integrity through histone acetylome refinement during early embryogenesis. BioRxiv. 10.1101/2022.05.05.490762

Zhou S, Zawel L, Lengauer C, Kinzler KW, Vogelstein B. Characterization of human FAST-1, a TGF beta and activin signal transducer. Mol Cell. 1998 Jul;2(1):121–7. [PubMed: 9702198]

Zhou Y, Zhou B, Pache L, Chang M, Khodabakhshi AH, Tanaseichuk O, Benner C, Chanda SK. Metascape provides a biologist-oriented resource for the analysis of systems-level datasets. Nat Commun. 2019 Apr 3;10(1):1523. [PubMed: 30944313]

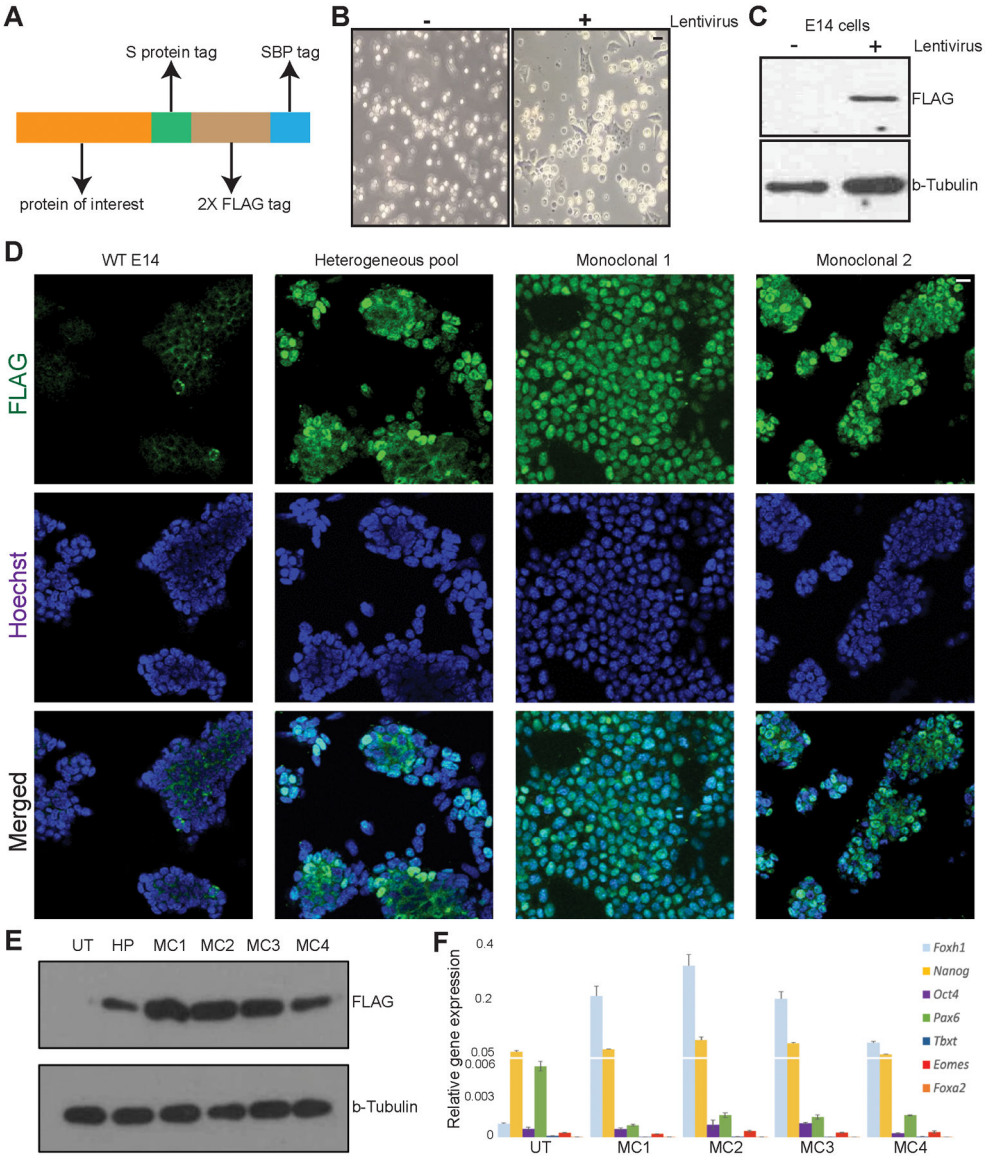

Figure 1: E14 mESCs stably expressing recombinant mFOXH1-SFB.

(**A**) A diagram of the recombinant protein with SFB triple tags, S-protein, FLAG, and streptavidin-binding peptide (SBP) at *C*-terminus. (**B**) E14 cells transduced by lentivirus after puromycin selection. Black scale bar: 10 microns. (**C**) Western blot of E14 cells expressing mFOXH1-SFB recombinant proteins using anti-FLAG antibody. β-Tubulin: loading control. (**D**) Immunofluorescence images of mFOXH1-SFB localized to the nucleus of E14 cells. The cytosolic signals of FLAG represent background. White scale bar: 10 microns. (**E**) Western blot showing the protein levels of mFOXH1-SFB in control E14 (UT), heterogeneous cell pool (HP), and monoclonal line MC1, MC2, MC3 and MC4. mFOXH1: anti-FLAG antibody; β-Tubulin: loading control. (**F**) RT-qPCR analyses of pluripotent and early germ layer markers in E14 mFOXH1-SFB cells. These gene expression levels were normalized to *gapdh*. Error bars: standard deviation values between two technical replicates.

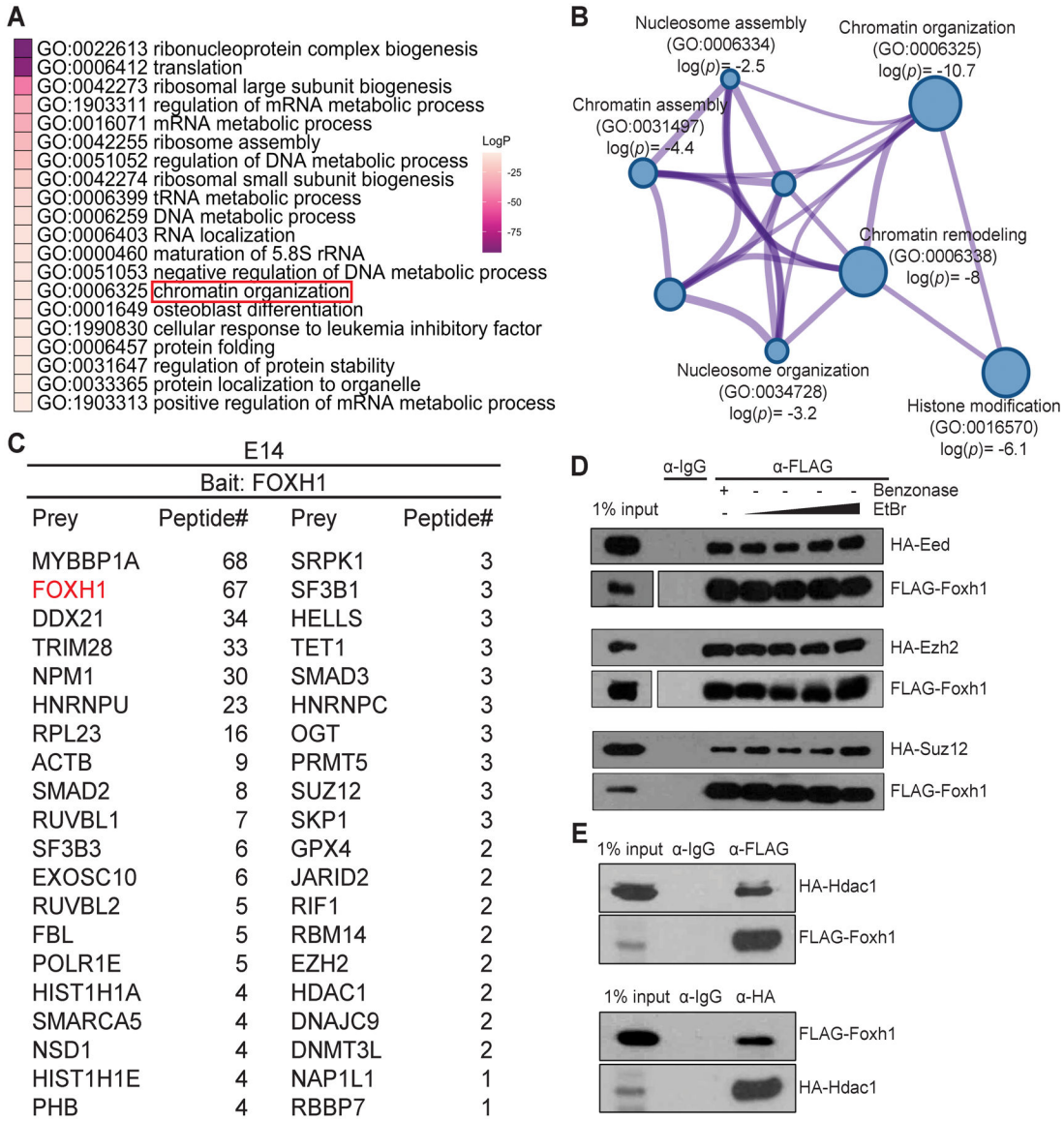

Figure 2: Foxh1 interacts with PRC2 subunits and Hdac1.

(**A**) Gene ontology enrichment analysis of 342 potential putative Foxh1 interacting proteins. (**B**) Interactome diagram illustrating Foxh1 interacting proteins in chromatin regulation in Cytoscape (Shannon et al., 2003). The sizes of circles reflect p-values. (**C**) The list of FOXH1 interacting proteins belonging to chromatin organization (GO:0006325), SMAD2, and SMAD3. The numbers indicate the mean of total peptides detected among three biological replicates. (**D**) Western blot showing the interaction between Foxh1 and PRC2 core subunits Ezh2, Eed, and Suz12 in HEK293T cells. EtBr: ethidium bromide. (**E**) Interaction between Foxh1 and Hdac1 in HEK293T cells.

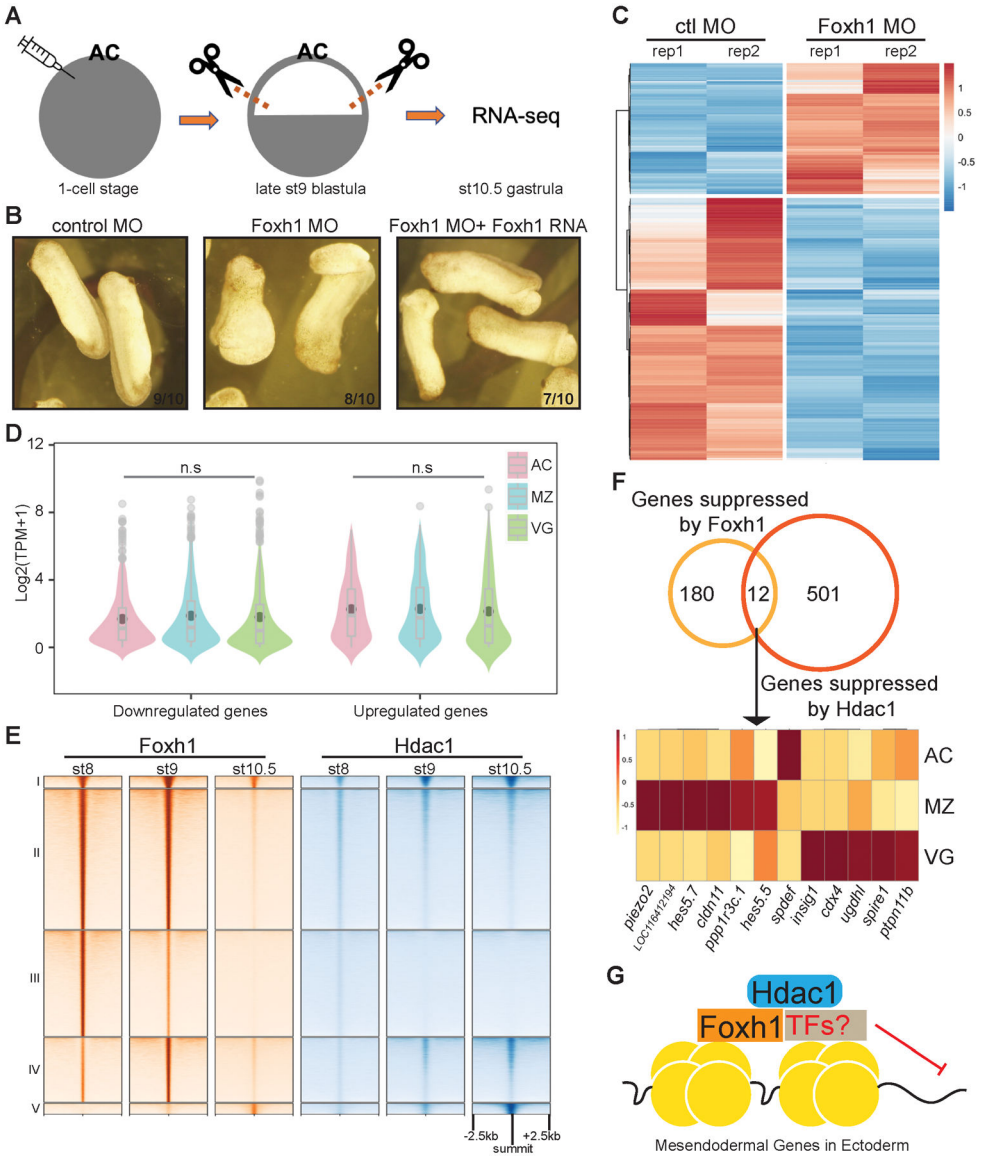

Figure 3: Mesendodermal gene suppression in the ectoderm by Foxh1-Hdac1.

(**A**) Dissection of animal cap for RNA-seq. (**B**) Foxh1 morphants and rescued embryos. Numbers of embryos with the representing phenotype are listed. (**C**) The heatmap representing differentially expressed genes in Foxh1 morphant versus control ectodermal tissues. (**D**) Violin plot showing the expression levels of Foxh1 regulated genes in different germ layers. AC: animal cap, MZ: marginal zone, and VG: vegetal mass. (**E**) Clustered heatmaps depicting the genomic binding signals of Foxh1 in st8 (mid blastula), st9 (late blastula), and st10.5 (early gastrula) embryos with a 5 kb window. Signals are centered on Foxh1 peak summits. (**F**) Venn diagram showing genes co-repressed by Foxh1 and Hdac1 in the ectoderm. The expression levels of 12 repressed genes in each germ layers are represented in the heatmap. (**G**) Model of Foxh1 and other unidentified TFs recruiting Hdac1 to suppress the mesendodermal gene regulatory program in the ectoderm.

Table 1:

342 high confidence interacting proteins identified from mass spectrometry

MYBBP1A	MTDH	RPS15A	HNRNPA3	SSB	SRSF6	GNAI2	HIST1H1E
TRIM28	ACTB	KPNA2	EBNA1BP2	MCM5	RBM28	JARID2	ABCF2
NCL	PABPC1	PNPLA6	RPS19BP1	ZSCAN4C	DHX37	IMP3	DNAJC21
HNRNPU	RPL8	ATP5C1	HNRNPC	EXOSCIO	IARS	DNMT3L	POLR2A
HSPA8	SYNCRIP	EPRS	RFC4	ATP1A1	TCP1	POLR2E	RPF2
HSP90AB1	HNRNPH1	RPS24	ATP2A2	FRG1	RTCB	SPTLC1	MRPS30
HNRNPM	PTBP1	MDN1	NOL6	SKP1	URB2	DUS3L	HDAC1
RPL7	TDH	RPL21	DDX28	RBMXL2	ALYREF	RPLP1	AP2A2
RPS4X	CKAP4	GLYR1	SRSF3	C1QBP	TUBB4B	PISD	LARP7
ATAD3	DDX1	ABCE1	MYEF2	DDX47	RPL34	PPAN	AP2M1
DDX21	UTP20	RUVBL1	PRDX1	ESC02	NARS	TMEM214	SPTLC2
RPL4	NAT 10	RPS7	TARDBP	HSPD1	RPL35	RRP15	CDIPT
TRIM71	RCC2	CAD	POLR1B	FAM98B	VCP	DNAJB6	CCT3
PDCD11	RRP12	RPL26	TRIM25	SLC25A1	SSR1	HSP90B1	TRIP12
FOXH1	HSPA2	RPS26	PES1	RPS27	NSUN2	CANX	FAU
RPS9	RPL23A	RPL14	SGPL1	L1TD1	SMAD2	NOL9	DDX49
LBR	RPL18	RPL18A	VDAC2	NOP53	RPN2	YBX3	MRPL39
GNL3	NOP2	YBX1	RPL22	EXOSC9	NOP16	MRPL15	GTF3C1
RPS2	RPL30	SERBP1	POLR1E	RBM39	TIMM23	CFL1	MRPS26
DDX5	RPL27	RPLP2	AP2B1	DDX10	HNRNPAB	RSL24D1	IGF2BP3
RPL6	DRG1	ASPH	DNAJA3	RPL36-PS3	PCBP3	DDX27	RBBP7
D1PAS1	DNAJA1	CSDE1	TECR	RUVBL2	LYAR	TUBA4A	ERLIN2
NOP56	MCM3	HK2	ILF2	RRP1B	BCAS2	CUL1	PRMT5
RPL7A	RARS	RPL19	GNL3L	RBM19	ARMC10	PTCD3	STAU1
RPL3	RSL1D1	HELLS	RPL17	NOP14	WDR46	RPS19	TEX10
RPS6	DDX17	DARS	CAPRIN1	RFC2	NIFK	FUS	EIF2S3Y
RPL10A	PRPF19	RACK1	RPL10L	DDX56	SRPK1	SMAD3	CEBPZ
RPS11	DHX15	TSR1	PFKP	MRPL21	NAP1L1	DDOST	PCBP1
RPL13	EIF2S2	RPSA	KPNB1	RFC5	AIMP1	GRSF1	NEMF
RPL13A	TUFM	ABCF1	NXF1	SLC25A3	NISCH	G3BP1	POLRMT
IGF2BP1	DDX51	SUZ12	NOP58	RPL27A	RFC1	GPX4	RARS2
RPL23	RPL24	POLR1C	EXOSC8	RBMX	EZH2	XRN2	MSH6
YME1L1	HDLBP	FXR1	ANKRD17	WDR18	DDX52	DDX31	OGT
CDC5L	POP1	RPS20	HNRNPR	PHB	HNRNPD	RPS28	TRMT1L
NPM1	DHX30	SLC25A5	HNRNPAO	GTPBP4	SRPRB	SMARCA5	TET1
RPS18	FBL	TIMM50	RPS4L	CD3EAP	RRBP1	RBM14	PDE12
HNRNPF	RPL35A	HNRNPA1	NVL	AIFM1	CCT4	ZFR	HIST1H1A
RPS16	RPL31	MTCH2	LAS1L	SLC25A13	FKBP8	NSD1	MSH2

RPS13	RPS25	RPL15	RBFOX2	SF3B1	GTPBP1	KARS	RIF1
HSD17B12	HSP90AA1	DHX9	MARS	FTSJ3	RPL37A	PRKCI	LENG8
SPATA5	RPL10	RBM34	ILF3	AFG3L1	DNAJA2	SLC25A4	POLR1A
RPLPO	RPS8	TUBB4A	SF3B3	SENP3	EEF1G	SRSF4	
TMPO	RPS23	RPN1	EIF4A2	CDKAL1	AIMP2	DNAJC9	